COMMUNICATION

Bulky toroidal and vesicular self-assembled nanostructures from fullerene end-capped rod-like polymers†

D. Mazzier, M. Mba, M. Zerbetto* and A. Moretto*

In this work, we present novel fullerene (C_{60}) end-capped rod-like polypeptide-polymers, obtained by one-pot thiol–ene chemistry. These systems are able to self-assemble in water creating precise bulky microstructures of toroidal or vesicular shapes. Independent molecular dynamics simulations supported the observed experimental results.

One of the novel themes in areas such as materials science, nanochemistry and biomimetic chemistry is the construction of supramolecular architectures characterized by well-distinct shapes and functions.[1,2] Undoubtedly, the self-assembly process of polymers through non-covalent interactions, including hydrophilic and hydrophobic effects, electrostatic contacts, hydrogen bonding, microphase segregation and shape effects, has great potential for creating such supramolecular architectures.[3–6] Recently, the improvement in synthetic methodologies associated with the use of designed conformational constraints led to the ability to perform nanometric control, on both size and shape, even at the single polymer molecule level.[7] In the literature many examples of supramolecular vesicles and micelles formed by block copolymers containing at least one high-molecular weight polymeric peptide domain,[8–10] as well as by small- or medium-sized peptides conjugated with molecules of nonpeptidic nature,[9,11] can be found. Rarely, homo-polypeptides alone were reported as precursors of self-assembled microstructures that are spherical in shape. Polypeptides prepared by the ring-opening polymerization (ROP) of α-amino acid *N*-carboxyanhydrides (NCAs), which have been known since many decades,[12] are nowadays emerging biomaterials[13] that are gaining increasing attention for various applications including drug delivery, gene therapy, antibiotics and tissue engineering.[14] Polypeptides can offer considerable chemical diversity: beyond the twenty canonical amino acids alone, non-canonical amino acids are readily accessible

from commercial sources or could be designed and synthesized depending on the finalities. Moreover, polypeptides are fascinating and unique due to their ability to self-assemble into ordered structures,[15] making them attractive in those many applications where well-organized architectures are essential to accomplish a function. Substantial progresses have been made in the NCA/ polypeptide field in the past decade[14] and today several innovative polypeptide-based materials have been produced and studied.[16] Apart from the ability to assemble in a wide range of different supramolecular structures of nanoscale dimensions,[17] another unique characteristic of rod-polypeptidic segments is the possibility to endow various functionalities such as photophysical and electrochemical properties to the supramolecular materials. An example of a well-known rod-like polypeptide is poly(γ-benzyl-ʟ-glutamate) (PBLG). PBLG has intramolecular hydrogen bonds that stabilize the secondary α-helical structure and shows mesoscopic liquid crystal order because of its good solubility and rod-like structure.[18] Inspired by the recent work of Yagci and co-workers,[19] we decided to functionalize both N- and C-termini of PBLG using thiol–ene chemistry[20] to prepare C_{60}–PBLG (C_{60}, fullerene) conjugates in a way that only C or C/N-terminus mono-addition products are formed without any contamination of ill-defined derivatives. In particular, herein we report the one-pot synthesis of two C_{60}–PBLG derivatives, namely NH_2–PBLG–C_{60} (**3**) and C_{60}–PBLG–C_{60} (**6**) (Fig. 1) and their controlled self-assembly in water.[21]

Department of Chemical Sciences, University of Padova, Via Marzolo 1, 35131 Padova, Italy. E-mail: alessandro.moretto.1@unipd.it, mirco.zerbetto@unipd.it

† Electronic supplementary information (ESI) available: Synthetic details, SEC traces, ^{13}C-NMR, ^{1}H-NMR and solid state IR characterization of the polymers (**1**, **3** and **6**). See DOI: 10.1039/c4cc01477d
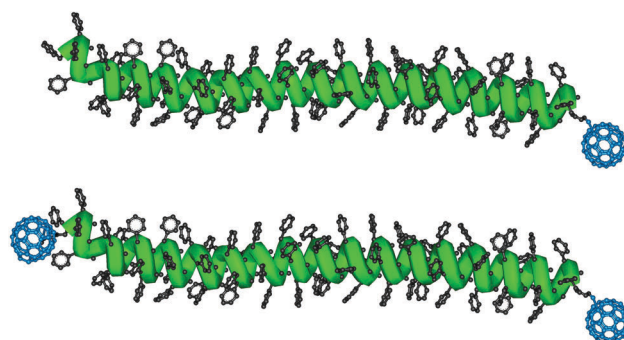
Fig. 1 Molecular structures of NH_2–PBLG–C_{60} (**3**) and C_{60}–PBLG–C_{60} (**6**).
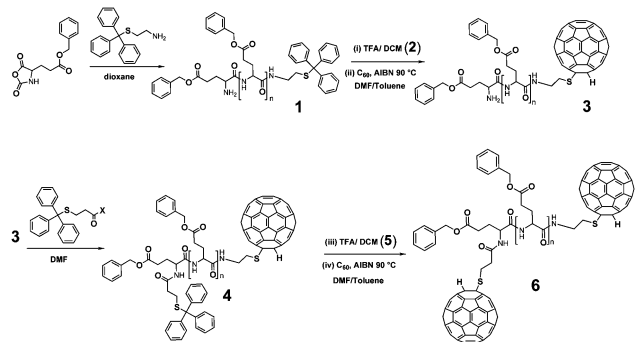
Scheme 1 Synthesis of polymers NH_2–PBLG–C_{60} (**3**) and C_{60}–PBLG–C_{60} (**6**).

BLG–NCA (4 mmol) was polymerized in dioxane for 24 h at room temperature, using Trt-cysteamine (Trt, triphenylmethyl) as the initiator (0.04 mmol) (Scheme 1). Polymer **1** was obtained after precipitation with methanol in 81% yield (M_W = 19 100 and PDI 1.11 by SEC). Subsequently, the Trt-protecting group was removed yielding polymer **2** (not shown in Scheme 1). Next, **2** (0.01 mmol) was dissolved in DMF and added to toluene. Then, fullerene (0.05 mmol) and AIBN (0.15 mmol) were added (in this order) to the previous solution and the subsequent homogeneous mixture was heated at 90 °C under stirring for 5 h. Subsequently, the solvent was removed and the resulting solid was suspended in DMF, passed through a 20 μm filter, and then precipitated by addition of methanol, giving polymer **3** as a brown solid in 85% yield (M_W = 19 550 and PDI 1.09 by SEC).

Moreover, polymer **3** was successively N-end capped with a large excess of pre-activated Trt-mercaptopropionic acid, yielding polymer **4** (not shown in Scheme 1). Polymer **4** was C-terminus Trt-deprotected (as described before, yielding polymer **5**, not shown in Scheme 1) and placed to react under the same conditions described above for the synthesis of polymer **3**, thus to generate the bisconjugate C_{60}–PBLG–C_{60}, polymer **6** in 78% yield (M_W = 20 300, PDI 1.11 by SEC). Since all the synthesized polymers possess the same PBLG part (as it comes from polymer **1**), the differences in M_Ws determined by SEC constitute a first evidence for the addition of one or two fullerenes.

A second evidence for the covalent attachment of fullerenes arises from the absorption spectra of **1**, **3** and **6**, which were recorded in a THF solvent and are shown in Fig. 2A. The observed patterns are close to that of fullerene, which shows high UV absorptions at around λ = 287 and 330 nm and tails spanning over the 600 nm

region. We assign the observed UV absorptions in **1** and **2** mono and bis fullerene-conjugates to the fullerene moiety[19] considering the small differences in the resonance frequencies with respect to the isolated fullerene due to perturbations of the electronic structure caused by the bonding with the PBLG polymer. The third indication of the formation of PBLG-conjugated fullerenes comes from the thermal stability of **1**, **2** and **3** that was investigated *via* thermogravimetric analysis (TGA; 100–700 °C) under nitrogen flow with a heating rate of 10 °C min^{-1} (Fig. 2B). Accordingly, PBLG polymers undergo thermal decomposition between 250 and 350 °C, whereas the thermally stable fullerene component maintains its stability up to almost 600 °C.[19] The weight percentages of the components (polymer **3**, C_{60}/PBLG 4:96%; polymer **6**, C_{60}/PBLG 7:93%) determined by TGA are in agreement with those of SEC analysis. All of the experimental results suggested an average number of BLG amino acids, for the polymer unit, close to 85. The secondary structure of polymers **1**, **3** and **6** was analyzed by ECD (electronic circular dichroism), which confirmed the preservation of the α-helical conformation for all the synthesized compounds (Fig. S1, ESI†), which in turn implies the rod-like shape of the polymers. Synthetic details, SEC traces, ^{13}C-NMR, ^{1}H-NMR (the last two characterizations do not allow the detection of C_{60} due to the large amount of PBLG with respect to C_{60}) and solid state IR characterization of the polymers (**1**, **3** and **6**) are reported in the ESI† and Fig. S2–S5, respectively.

From polymer **3**, donut-like morphologies were generated, in the form of a milk-like suspension, starting from a 20 mg (3:7, v/v) DMF–THF solution (10 mL) dialyzed (membrane cutoff, 12 KD) against ultrapure water (48 hours) (Fig. 3).

TEM (transmission electron microscopy) images show toroidal shapes with an external diameter ranging between 200 nm and 650 nm (Fig. 3A and B, stained and unstained samples, respectively), additionally confirmed by SEM (scanning electron microscopy) analysis (Fig. 3C). Moreover, AFM (atomic force microscopy) details of the selected nanodonut shown in Fig. 3C reveal a diameter of 200 nm, a thickness of

Fig. 3 (A and B) TEM (A, stained and B, unstained) images of the resulting self-assembled nanostructures obtained from polymer **3**. (C) SEM image from the very same prepared sample used in TEM analysis. (D and E) AFM micrograph and high-profile of the selected (1) toroidal nanostructure.

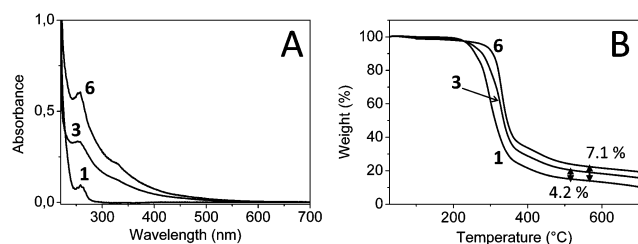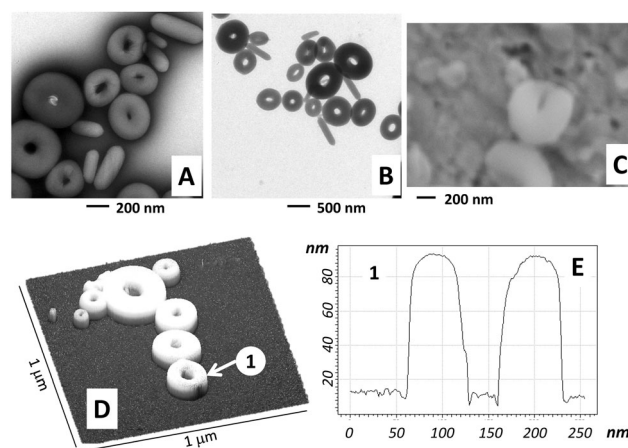**Fig. 2** (A) UV/Vis spectra of polymers **1**, **3** and **6** in THF solution (concentration: 0.01 mg mL^{-1}). (B) Thermogravimetric analysis comparison of polymers **1**, **3** and **6**.
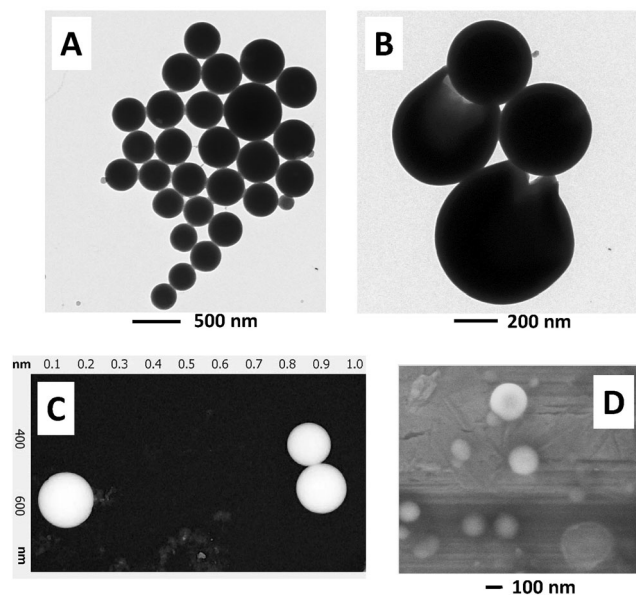
Fig. 4 (A and B) TEM (unstained) images of the resulting self-assembled nanostructures obtained from polymer **6**. (C and D) AFM and SEM images, respectively, from the very same sample used for TEM analysis.

70 nm and a hole of 30 nm (Fig. 3D). Additionally, after running the same self-assembly process but starting from a more diluted solution of **3** (2–5 mg in 10 ml), smaller but uniform in size (60 nm diameter), toroidal nanostructures were obtained as detected by AFM (Fig. S6, ESI†). Sphere-shaped aggregates were generated from polymer **6** under the same conditions described above for polymer **3** (Fig. 4). TEM, unstained, images reveal the formation of deep-dark and round morphologies (Fig. 4A) with diameters ranging between 250 and 700 nm. Moreover, these aggregates displayed an internal cavity as shown in the TEM image in Fig. 4B; thus, the observed spherical morphologies can be attributed to hollow vesicle-like microstructures. These results were additionally confirmed by AFM (Fig. 4C) and SEM analyses (Fig. 4D). While polymers **3** and **6** were able to self-assemble into ordered structures, polymer **1**, bearing a Trt group instead of fullerene, did not give any specific nano-structuration under similar conditions. To get polymer **3** from **1**, the Trt protecting group was removed under acidic conditions, thus in polymer **3** the N-terminus amine is protonated (NH_3^+). Importantly, when NaOH 0.2 M was added to a solution containing the toroidal objects obtained by the self-assembly of **3**, immediate precipitation of the polymer was observed. On the other hand, the addition of 0.2 M HCl did not affect the self-assembled structures, since donut-like structures could still be detected by TEM. This information suggested that: (i) fullerene is necessary for the formation of ordered nanostructures and (ii) the NH_3^+ group is mandatory for the formation of the toroid-shaped structures.

Since, at a fixed volume, a toroidal shape exposes a larger surface with respect to the spherical shape, our hypothesis is that to generate self-assembled toroidal forms in water (starting from the hydrophobic polymer **1**) the single polymer chain may firstly undergo a tail-to-tail dimerization and successively a large scale, coil–coil spiral-like, self-assembly process. According to this hypothesis, all of the fullerenes could be aligned along an internal axle, thus to result buried by the PBLG hydrophobic helices, while the charged NH_3^+ groups may be exposed to water solution (a schematic representation is shown in Fig. S7, ESI†) in accordance with previously reported similar, but much smaller, structures.[22] This hypothesis is in agreement with the pH-depending experiments described above. Moreover, the same but shorter functionalized PBLG-polymer series was also synthesized using a BLG–NCA/initiator ratio of 25 : 1. After the self-assembly assay, the shorter **1** and **3** analogues did not provide any specific microstructure propensities while the shorter **6** analogue afforded smaller spherical structures (10–35 nm diameter) compared to the previously described (Fig. S8, ESI†).

Calculus was used to support experimental observations and in particular to investigate the atomistic structure of the vesicles formed by polymer **6**. To this purpose we employed a bottom-up coarse-graining protocol with the intent to set up a simulation able to independently recover the experimental observations, *i.e.* we did not use the experimental results to bias the parameterization of the model. To limit the computational weight of the whole procedure we used polymer **6** constituted by 25 BLG units as a model molecule. The coarse-graining representation sees each of the BLG units and the two terminal moieties as single beads. Differently from systems recently reported in the literature,[23] in which a balance between attractive and repulsive forces of the building blocks drives the assembly, here the driving force of the self-assembly is the low affinity of the hydrophobic PBLG molecules with water. Thus, in our simulations we needed to include explicitly the medium to observe aggregation of polymer **6** molecules. We employed a coarse-grained 4-water model for the solvent, in which one bead is used to represent a cluster of 4 water molecules.[24,25] Details on the coarse graining procedure and the parameterization of the bead–bead energy function are provided in the ESI.† We simulated a system containing 1600 polymer molecules and 1 600 608 water beads (see the ESI† for details). The starting configuration, in which the polymer molecules are randomly placed and oriented in space, is shown in Fig. 5A (water was omitted for clarity).

The situation just after 5 ns of simulation time is shown in Fig. 5B. The simulation box results are populated by a small number of aggregates with different shapes. Most of them are spherical aggregates of dimensions ranging from 15 to 20 nm in diameter. However, a couple of assemblies are present which show a bent layer of about 4 nm thickness (very close to the length of one polymer molecule) that can be thought to be a piece of a larger vesicle that could not be formed in this simulation due to an insufficient number of polymer molecules. A number of important observations can be drawn from the simulations. The first and most important observation reflecting the experiments is that in water the polymer molecules aggregate into ordered structures instead of forming an amorphous precipitate. Second, all the aggregates are formed by layers of limited size ranging from 4 to 6 nm, which is in the order of the length of the polymers. Third, the layer is not structured in a simple way as it happens in phospholipids:
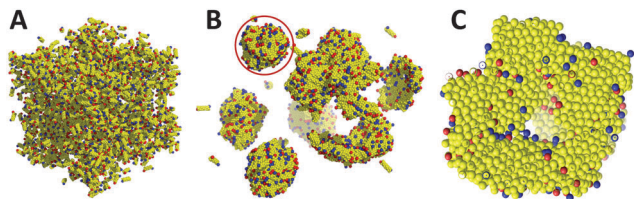
Fig. 5 The color scheme is: yellow represents BLG beads, red for the N-terminal group, and blue for the C-terminal group. Beads radii are set to 0.43 nm for the BLG units and 0.53 nm for the terminal moieties. These values have been determined from the average translational diffusion tensor of moieties calculated using a hydrodynamic approach.[26] Water molecules have been omitted for clarity. (A) Initial random configuration of the 1600 PBLG molecules constituted by 25 BLG amino acids. (B) Final configuration of the system after 5 ns of simulation time. (C) Details of a selected spherical aggregate with front and rear clipping planes applied to highlight the hollow part of the spherical aggregate.

couple of polymers form coiled-coil super structures, which in turn create a network giving rise to the layer, with the C_{60} termini preferentially exposed to the solvent. We shall also notice that, while being quite compact, the spherical structures obtained in the simulation are hollow (Fig. 5C). The obtained aggregates are in quite good accord with those observed experimentally for the shorter **6** analogue.

In this work, we reported the one-pot synthesis of two novel PBLG-polymers, C- and C/N-terminus capped with fullerenes, by means of thiol–ene chemistry. The self-assembly of such rod-like systems in water led to the formation of bulky, toroid-like or vesicle-like, nanostructures depending on the fullerene position over the main chain of the polymer. Based on experimental results, we suggested a mechanism for the formation of the toroidal nanostructures and we explored vesicle-like systems by means of computational modelling. In conclusion, such polymer–fullerene conjugates may be interesting systems to prepare organized, at a nanoscale level, fullerene-based devices.

Notes and references

1 A. R. Hirst, B. Escuder, J. F. Miravet and D. K. Smith, *Angew. Chem., Int. Ed.*, 2008, **47**, 8002.

2 G. M. Whitesides and M. Boncheva, *Proc. Natl. Acad. Sci. U. S. A.*, 2002, **99**, 4769.

3 G. M. Whitesides and B. Grzybowski, *Science*, 2002, **295**, 2418.

4 O. Ikkala and G. ten Brinke, *Science*, 2002, **295**, 2407.

5 J. A. A. W. Elemans, A. E. Rowan and R. J. M. Nolte, *J. Mater. Chem.*, 2003, **13**, 2661.

6 V. Percec, C.-H. Ahn, G. Ungar, D. J. P. Yeardley, M. Möller and S. S. Sheiko, *Nature*, 1998, **391**, 161.

7 P. J. M. Stals, Y. Li, J. Burdyńska, R. Nicolaÿ, A. Nese, A. R. A. Palmans, E. W. Meijer, K. Matyjaszewski and S. S. Sheiko, *J. Am. Chem. Soc.*, 2013, **135**, 11421.

8 Recent reviews: (*a*) G. Fuks, R. M. Talom and F. Gauffre, *Chem. Soc. Rev.*, 2011, **40**, 2475; (*b*) S. F. M. van Dongen, H.-P. M. DeHoog, R. J. R. W. Peters, M. Nallani, R. J. M. Nolte and J. C. M. van Hest, *Chem. Rev.*, 2009, **109**, 6212; (*c*) E. Soussan, S. Cassel, M. Blanzat and I. Rico-Lattes, *Angew. Chem.*, 2009, **121**, 280; E. Soussan, S. Cassel, M. Blanzat and I. Rico-Lattes, *Angew. Chem., Int. Ed.*, 2009, **48**, 274.

9 Recent reviews: (*a*) Z. Luo and S. Zhang, *Chem. Soc. Rev.*, 2012, **41**, 4736; (*b*) C. Valéry, F. Artzner and M. Paternostre, *Soft Matter*, 2011, **7**, 9583; (*c*) X. Yan, P. Zhua and J. Li, *Chem. Soc. Rev.*, 2010, **39**, 1877; (*d*) I. W. Hamley, *Angew. Chem.*, 2007, **119**, 8274–8295; I. W. Hamley, *Angew. Chem., Int. Ed.*, 2007, **46**, 8128–8295.

10 Recent reviews: (*a*) B. Tian, X. Tao, T. Ren, Y. Weng, X. Lin, Y. Zhang and X. Tang, *J. Mater. Chem.*, 2012, **22**, 17404; (*b*) C. Cai, L. Wang and J. Lin, *Chem. Commun.*, 2011, **47**, 11189; (*c*) A. Carlsen and S. Lecommandoux, *Curr. Opin. Colloid Interface Sci.*, 2009, **14**, 329.

11 (*a*) N. Gour, D. Kedracki, I. Safir, K. X. Ngo and C. Vebert-Nardin, *Chem. Commun.*, 2012, **48**, 5440; (*b*) H. Wang, C. Yang, L. Wang, D. Kong, Y. Zhang and Z. Yang, *Chem. Commun.*, 2011, **47**, 4439; (*c*) Y. Zhou, M. Kogiso and T. Shimizu, *J. Am. Chem. Soc.*, 2009, **131**, 2456; (*d*) S. Ghosh, M. Reches, E. Gazit and S. Verma, *Angew. Chem.*, 2007, **119**, 2048; S. Ghosh, M. Reches, E. Gazit and S. Verma, *Angew. Chem., Int. Ed.*, 2007, **46**, 2002.

12 R. B. Woodward and C. H. Schramm, *J. Am. Chem. Soc.*, 1947, **69**, 1551.

13 J. Huang and A. Heise, *Chem. Soc. Rev.*, 2013, **42**, 7373.

14 (*a*) H. R. Kricheldorf, *Angew. Chem., Int. Ed.*, 2006, **45**, 5752; (*b*) H. Lu, J. Wang, Z. Song, L. Yin, Y. Zhang, H. Tang, C. Tu, Y. Lin and J. Cheng, *Chem. Commun.*, 2014, **50**, 139.

15 T. O. Yeates and J. E. Padilla, *Curr. Opin. Struct. Biol.*, 2002, **12**, 464.

16 M. Zelzer and R. V. Ulijn, *Chem. Soc. Rev.*, 2010, **39**, 3351.

17 M. Lee, B.-K. Cho and W.-C. Zin, *Chem. Rev.*, 2001, **101**, 3869.

18 P. Doty, J. H. Bradbury and A. M. Holtzer, *J. Am. Chem. Soc.*, 1956, **78**, 947.

19 B. Iskin, G. Yilmaz and Y. Yagci, *Chem. – Eur. J.*, 2012, **18**, 10254.

20 C. E. Hoyle and C. N. Bowman, *Angew. Chem., Int. Ed.*, 2010, **49**, 1540.

21 (*a*) D. M. Guldi, F. Zerbetto, V. Georgakilas and M. Prato, *Acc. Chem. Res.*, 2005, **38**, 38; (*b*) V. Georgakilas, F. Pellarini, M. Prato, D. M. Guldi, M. Melle-Franco and F. Zerbetto, *Proc. Natl. Acad. Sci. U. S. A.*, 2002, **99**, 5075.

22 Y. Kim, W. Li, S. Shin and M. Lee, *Acc. Chem. Res.*, 2013, **46**, 2888.

23 C. Cai, Y. Li, J. Lin, L. Wang, S. Lin, X.-S. Wang and T. Jiang, *Angew. Chem., Int. Ed.*, 2013, **52**, 7732.

24 S. J. Marrink and A. E. Mark, *J. Am. Chem. Soc.*, 2003, **125**, 15233.

25 J. Marrink, H. J. Risselada, S. Yefimov, D. P. Tieleman and A. H. de Vries, *J. Phys. Chem. B*, 2007, **111**, 7812.

26 V. Barone, M. Zerbetto and A. Polimeno, *J. Comput. Chem.*, 2009, **30**, 2.